PROCEEDINGS, 44th Workshop on Geothermal Reservoir Engineering
Stanford University, Stanford, California, February 11-13, 2019
SGP-TR-214

Three-Dimensional Temperature Simulations of the Acoculco Caldera Complex, Puebla, Mexico

Fernando J. Guerrero-Martínez*, Rosa M. Prol-Ledesma, Eduardo J. Granados-Pastrana, Juan L. Carrillo-De La Cruz, Augusto A. González Díaz, Irving A. González-Romo

Institute of Geophysics, Universidad Nacional Autónoma de México, Cd. Universitaria, México D.F., 04510, México

*fguerrero@igeofisica.unam.mx

Keywords: Numerical modeling, Curie isotherm, Finite Volume

Abstract

Temperature simulations of the Acoculco caldera complex are undertaken to improve our understanding of its thermal regime. This volcanic caldera has been considered a Hot Dry Rock geothermal system based on evidences of low permeability of the formations hosting the heat source. A background heat flow in the area is modeled by means of an estimated Curie isotherm at depth which represents a constant temperature boundary condition. Additionally, local thermal anomalies are considered in the model. The description of the structures controlling the heat flow is based on limited borehole data along with geophysical surveys. The heat transfer equation is then solved in steady state with the Finite Volume method. The resulting computational model is intended to be an instrument to test assumptions on the thermal regime in the Acoculco caldera. Additionally, it is a framework to study the relation between heat flow measurements and the estimation of the Curie isotherm that can be applied to other study areas. In the case of the Acoculco caldera, the numerical results show that shallow and localized thermal anomalies (750 °C) are necessary to attain the high geothermal gradients that have been measured in the field. The thermal anomalies turn out to be between 3100 and 3400 m below ground surface, shallower than those assumed in previous 1D thermal models in this caldera complex.

1. INTRODUCTION

The Trans-Mexican Volcanic Belt (TMVB) is a promising region for the development of geothermal energy in Mexico, the volcanic province. There are currently three prominent geothermal fields in this region of the country: Los Azufres (248 MWe), Los Humeros (94 MWe), and Domo San Pedro (25 MWe) along with several prospective areas that have been explored in the past, such as La Primavera caldera and the Acoculco caldera (Ac) (Gutiérrez-Negrín et al. 2015). In particular, the Acoculco geothermal area has been considered a Hot Dry Rock geothermal system (Lorenzo-Pulido et al. 2011) since it combines high geothermal gradients (~138 °C/km) with low permeability formations.

Reservoir simulation is an important step in geothermal exploration to accomplish more accurate conceptual models and define exploitation strategies (Franco and Vaccaro 2012). In particular, it can be a powerful tool to test hypotheses made on the thermal regime of the system (Verma and Gómez-Arias 2016). The modeling process can be divided into three work stages: geology, geochemistry, and geophysics. As more field evidence is gathered from these stages the conceptual model can be more rigorously constrained. The numerical model has to reflect as much as possible the structural and physical considerations the conceptual model is based on. Subsequently simulation tests are carried out to evaluate how accurately the assumptions and field evidences are reproduced.

Due to limited subsurface data in the Ac, only 1D thermal modeling has been developed up to date (Avendaño-Cortés 2017, Canet et al. 2015a). These models are focused on describing the thermal regime and history of the exploratory wells rather than studying the entire caldera. In this work we attempt to simulate the 3D temperature field in the area using thermal conductivities of the lithological units that have been previously tested in the 1D models cited before. The model is calibrated with available temperature logs in the field. Currently there exist a variety of simulation tools to undertake this kind of modeling (see for instance the work by Thiery et al. (2018) and Finsterle et al. 2017). In this work we opted for developing a Finite Volume numerical scheme implemented in Fortran 90 that satisfies our assumptions and that has been tested in a previous case study (Gerrero-Martínez and Verma 2013). Basic assumptions for the conceptual model are the following: 1) The heat transfer occurs by conduction; 2) There exists an isotherm at depth (~580 °C) that can be estimated from aeromagnetic surveys in the region (Curie isotherm); 3) There exist local thermal anomalies within the caldera associated with the most recent volcanism; 4) Far from the local thermal anomalies the heat flow takes place in the vertical direction only, so that the lateral boundaries of the study area behave as adiabatic boundaries; 5) Radiogenic heat generation is negligible.

The model presented here is the first attempt to assess the thermal regime of this area in three dimensions and it allows us to get insight on the location and distribution of the heat source. The results show that under a conductive thermal regime, having multiple –distributed- heat sources at a constant temperature of 750 °C, a shallow depth of the sources is necessary to attain the observed geothermal gradients in the field: between 3100 and 3400 m below ground surface (bgs). Increasing the depth of these sources would require deep convective heat transfer (>2 km) if the geothermal gradients are to be maintained in the order of 138 °C/km.

2. GEOLOGICAL SETTING

The Ac is located in the state of Puebla, Mexico, on the east portion of the TMVB (Figure 1). It lies within a region affected by a NW-SE trending extensional deformation that has been accommodated by NE-SW trending normal faults (García-Palomo et al. 2018). The caldera collapse occurred at 2.7 Ma with the eruption of the Acoculco ignimbrite (>20 km^3), however volcanism has been active until 60 ka with late post-caldera eruptions of about 70 km^3 (Sosa-Ceballos et al. 2018). Several field campaigns between 2017 and 2018 have permitted us to identify other volcanic products (Figure 2), these include dacites, rhyolitic tuffs, andesitic and basaltic lavas. According with Sosa-Ceballos et al. (2018) the most recent eruptive products correspond to caldera margin and extra-caldera units (0.9 to 0.06 Ma). The study area contains up to 900 m of calcalkaline rocks overlying a Mesozoic sedimentary basement (Figure 2). The basement consists of a sedimentary sequence of the Sierra Madre Oriental which is composed of folded Cretaceous limestone and shales (López-Hernández et al. 2009). Viggiano-Guerra et al. (2011) presented a description of the lithology of the exploratory wells EAC-1 and EAC-2. As regards well EAC-1 (2000 m depth), the lithology can be divided into three sections from top to bottom: 1) Ignimbrites, dacites and rhyodacites (0-790 m); 2) Sequence of metamorphic rocks composed mainly by skarn and marble (790-1660 m); 3) The deepest section consists of a granitic body (>1660 m). On the other hand, the lithology of well EAC-2 can be grouped into the following sequence 1) Ignimbrites, dacites and andesites (0-340 m), 2) Altered and metamorphosed limestones (340-450 m); 3) Hornfels (480-1580 m); 4) Granitic intrusion (>1580 m).

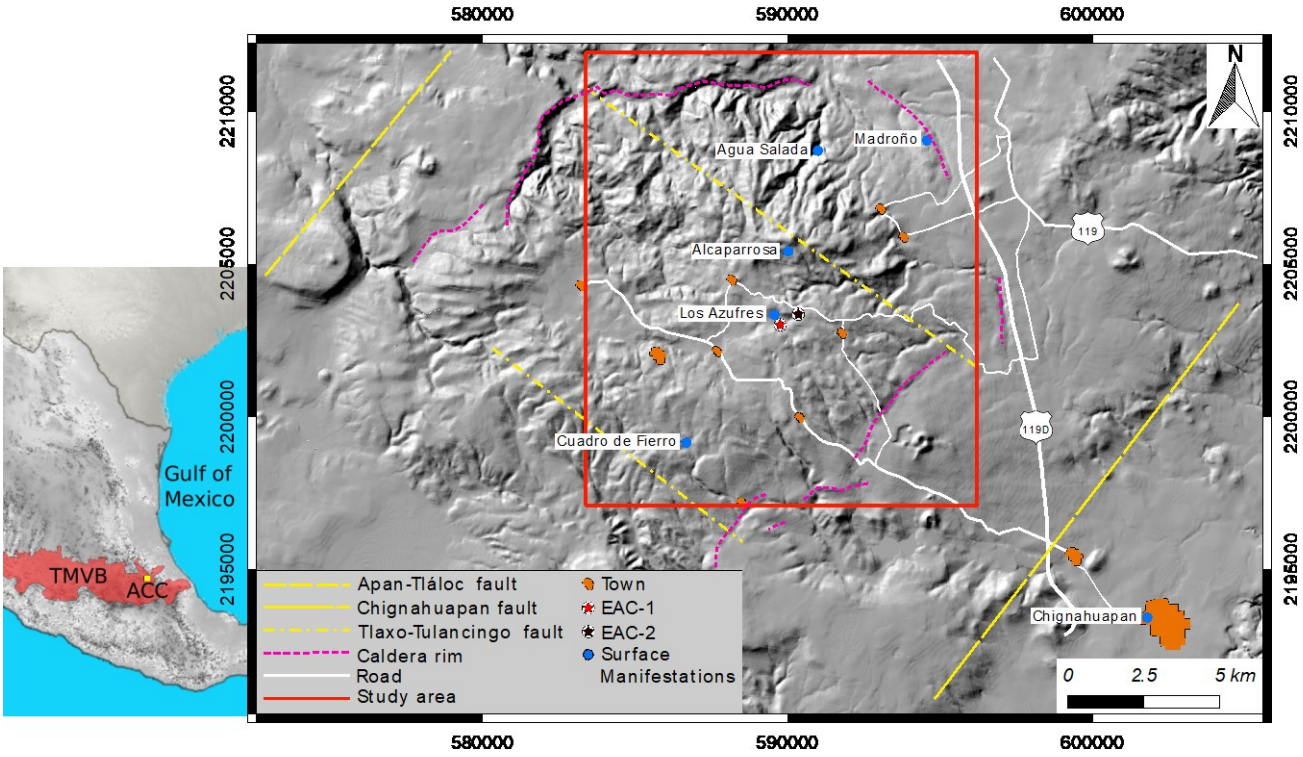

Figure 1: Location of the Acoculco caldera in the eastern portion of the Trans-Mexican Volcanic Belt (inferred caldera rim after Avellán et al. 2018)

3. EXPLORATORY WORK

The area is characterized by widespread hydrothermal alteration which extends down to a depth of 1000 m (Canet et al. 2015a). Surface hydrothermal manifestations within the caldera (Fig. 1) consist of bubbling springs and pools with close to ambient temperatures, soil degassing, and hydrothermally altered grounds. Temperature measurements in Agua Salada and Madroño (Fig. 1) were carried out in a field work campaign (November 2017), the locations consist of more than one spring or pond, the temperature ranges measured in these manifestations are the following: Agua salada, 4.9-23.6 °C; Madroño, 18.0-21.0 °C. Additionally, Peiffer et al. (2014) reported the following temperature ranges: Alcaparrosa, 12.2-15.0 °C; Los Azufres, 21.4-25.0; and Cuadro de Fierro, 23.0 °C.

The climate in the area is mild sub-humid with an average annual temperature of about 15 °C (Peláez-Pavón 2015). Water types in the study area are grouped into two main classes (Peiffer 2014): 1) sulfate-calcium composition with pH from acid to neutral at Alcaparrosa, Cuadro de Fierro, and Los Azufres and 2) near neutral pH bicarbonate-calcium-sodium at locations peripheral to the caldera complex (Chignahuapan, Quetzalapa, Jicolapa, El Rincón). The temperature of these springs range between 30 and 47 °C. High chloride content was measured at Chignahuapan which might be associated to a deep source of fluid mixed with shallow ground water (López- Hernández et al. 2009). Peiffer et al. (2014) pointed out that the acid and sulfate-rich character of the spring waters at Los Azufres and Alcaparrosa in comparison with peripheral waters could be related with the presence of a magmatic heat source. They suggest that magma reservoirs are located within the caldera, so that the higher solubility of H_2S in comparison with CO_2 can be the cause of the different water character at these manifestations.

As regards the geothermal gases the flux ranges reflect the low permeability of the shallow formations. In relation with this, Canet et al. (2015b) looked into the cessation of convective transport in the caldera and estimated from 1D thermal modeling that the decrease of permeability in the area started ~7000 years ago and took place in the upper 1400 m of the lithologic column. This cessation led to the present conductive thermal regime that has been observed in the temperature logs of wells EAC-1 and EAC-2.

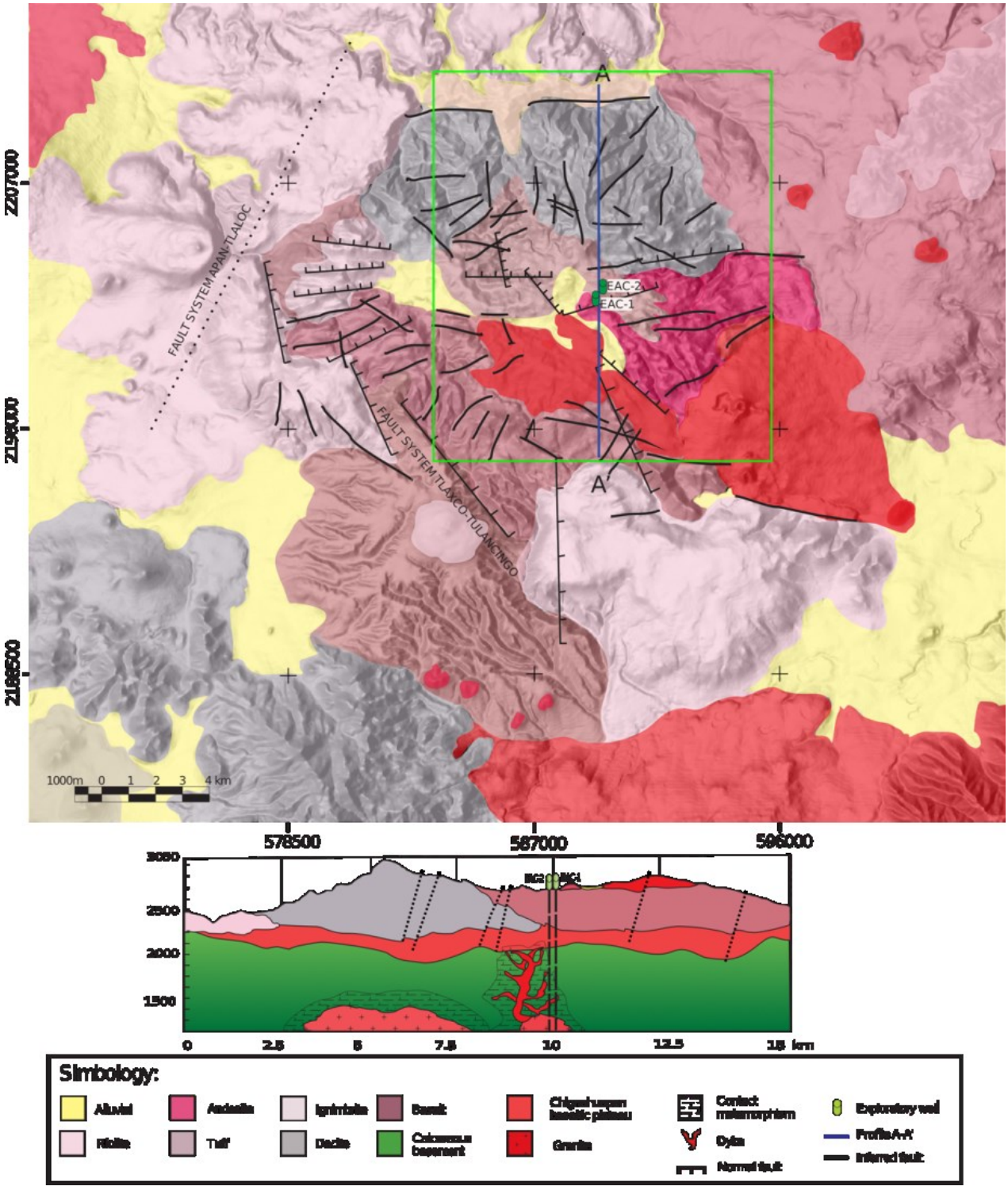

Figure 2: Geologic map of the Acoculco caldera. The study area for conceptual modeling is enclosed by the green rectangle.

López-Hernández et al. (2009) summarizes early geophysical exploration in the area. Gravity surveys show that the Ac lies within a general gravity low anomaly altered by the presence of several separate positive anomalies related to high-density intrusive rocks (for figures refer to the work cited). This is consistent with the lithology of wells that intersected dikes and a deep granitic body (Viggiano-Guerra etal. 2011). The magnetic surveys also show that the Acoculco caldera coincides with a magnetic high, the source of which has

been interpreted as an intrusive body related with a vent of post-caldera magmatism. The high density and high susceptibility anomaly may represent a vent of post caldera magmatism. Geoelectrical surveys show an extensive low resistivity anomaly covering almost entirely the area, which has been associated with a shallow zone of hydrothermal alteration (López-Hernández and Castillo-Hernández 1997).

More recently Granados-Pastrana (2018) processed aeromagnetic data of the Ac provided by the Mexican Geological Survey. Aeromagnetic surveys allow for regional mapping of magnetic anomalies in a geographic area that can be related with the temperature increase with depth (e.g. Okubo 1985). The Curie point (~580 °C) is the temperature at which a magnetic mineral loose its magnetization (Stacey and Banerjee 1974). On this basis Granados-Pastrana (2018) estimated the Curie depth in the Ac and reported that the mean depth is about 7800 m bgs. Assuming a curie temperature of 580 °C, this leads to a geothermal gradient of about 74 °C/km, which is consistent with the tectonic setting of the TMVB.

Two exploratory wells have been drilled in the area by the Federal Commission of Electricity (CFE). Well EAC-1 was drilled in 1994 to a depth of 2000 m. Temperature logs in this well were promising for geothermal applications, being 307 °C at the bottom of the well, the formations however turned out to be impermeable. On the other hand, the exploratory well EAC-2 was drilled (2008) at about 500 m NE of well EAC-1 to a depth of 1900 m. Hydrothermal alteration analysis presented by Viggiano-Guerra et al. (2011) in drill cuttings of well EAC-2 indicates there has been a self-sealing process in this zone.

4. CONCEPTUAL MODEL

The study area (Fig. 1) consists of 13050 m in *x*-axis, 15030 m in the *y*-axis. Regarding the *z*-axis, the domain comprises 6000 m below sea level (bsl) and 3100 m above sea level (asl). These limits are given by the minimum Curie depth (Granados-Pastrana 2018) and maximum elevation, respectively. In order to model the thermal regime in this area it is necessary to describe the heat sources and the mechanisms by which the heat is transported. In this model it is assumed that conduction is the only heat transfer mechanism, in agreement with field observations such as low permeability at depth as well as linear temperature logs in exploratory wells (Viggiano-Guerra et al. 2011). As regards the heat source, a background heat flow for the study area was established from the estimated Curie isotherm (580 °C) reported by Granados-Pastrana (2018). Additionally, since the Curie isotherm represents only a regional thermal feature in the area, local heat sources associated with the most recent magmatism are considered in the model. This consideration is consistent with the findings reported by Sosa-Ceballos et al. (2018), who addressed the magma origin and processes in the caldera complex as well as the possible distribution and location of the magmas that maintain active the geothermal field. They estimated a pre-eruptive temperature of 780±20 °C and proposed a swarm of dikes and sills as a possible arrangement of postcaldera magmatism. Based on these considerations a “dikes” scheme is proposed in this conceptual model to reproduce local and distributed heat sources. Five cylinders are considered to model the presence of magmatic intrusions. Figure 3 shows a 3D sketch of the conceptual model in which the heat sources are represented by five thin cylinders. The cylinders have a constant-temperature of 750 °C, which is on the order of the estimated pre-eruption temperatures mentioned above and consistent with previous 1D models. Likewise, the cylinders share the same radius and height. As a final consideration regarding the heat input of the system it is also assumed that radiogenic heat generation negligible.

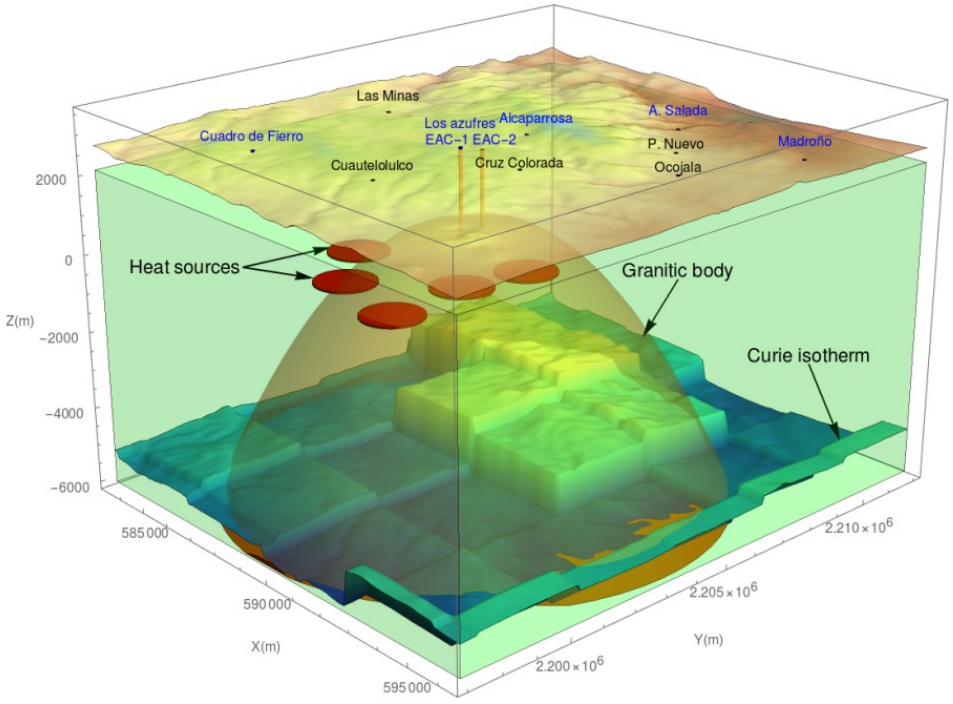

Figure 3: 3D sketch of the Ac geothermal system illustrating the estimated Curie isotherm and heat sources that give rise to the thermal regime in the area. The local heat sources are modeled by equal-size discs at a constant temperature of 750 ºC.

The distribution of rocks in the medium was built from the geological sections available and the lithology of wells (EAC-1 and EAC-2), which is the most detailed subsurface information available. Figure 4 shows a 2D schematic representation of the distribution of rocks in the model. The granitic intrusion intersected by both wells is represented by a parabolic-like surface that encloses the main portion of this intrusive body. The spatial distribution of the heat sources is chosen according with the evidences of high geothermal gradients in the exploratory wells along with the evidences of degassing of CO_2 and H_2S. Thermal conductivities of rocks are assigned taking as reference previous 1D thermal models presented by Canet et al. (2015b) and Avendaño-Cortés (2017) (Table 1). Although these 1D models are based on comprehensive reviews on thermophysical properties of rocks and calibration, both direct measurements and thermal recovery modeling in the exploratory boreholes (Wong-Loya et al. 2017) would be recommended to constrain more rigorously these parameters, unfortunately most of the drilling records of wells EAC-1 and EAC-2 remain as private reports. Further exploratory drilling becomes necessary to obtain a more accurate view of subsurface properties of rocks in this area.

As regards the boundary conditions, the topography and Curie isotherm act as Dirichlet boundaries with 15 °C and 580 °C, respectively. On the other hand, assuming that far from the thermal anomalies the heat flow takes place in the direction of z-axis, the lateral boundaries are defined as adiabatic boundaries.

Table 1: Thermal conductivities used in the conceptual model (Avendaño-Cortés 2017 and Canet et al. 2015b)

Rock	k (W/(mK))
Soils (air in pores)	0.80
Marl	2.80
Aplite	2.90
Skarn	1.60
Rhyodacite	2.08
Ignimbrite	1.65
Dacite	1.87
Tuff	1.40
Andesite	1.72
Limestone	2.60
Hornfels	2.50
Granite	2.20

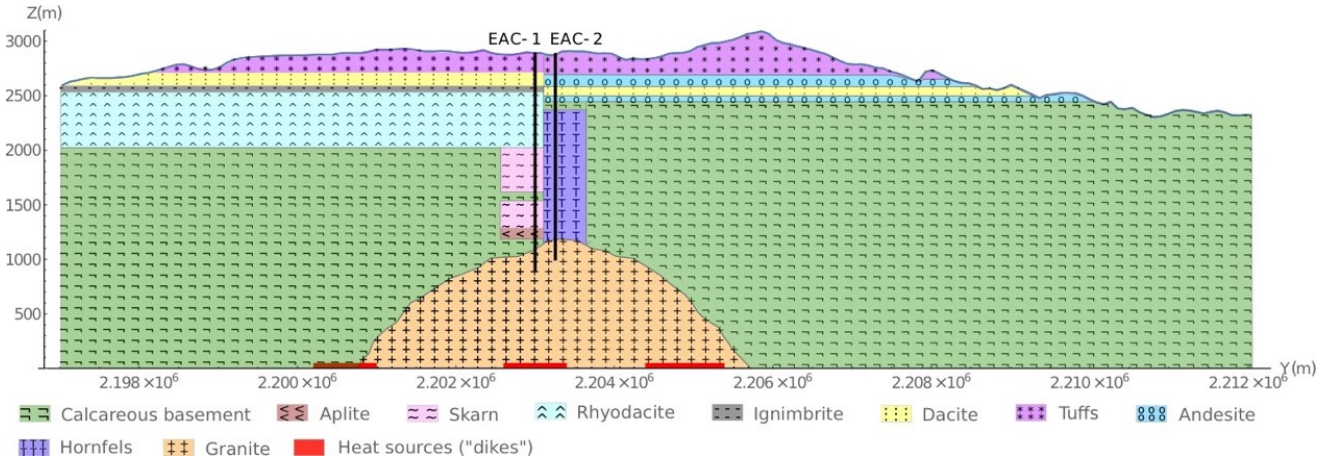

Figure 4: Simplified lithology of the Acoculco caldera (portion above the sea level at x=590000 m).

6. NUMERICAL MODEL

The steady-state heat transfer equation (Eq. 1) was discretized using a Finite Volume method (Versteeg and Malalasekera). A structured and uniform mesh was defined by Δx=Δy=90 m and Δz=25 m, this turns out about 15 times higher mesh resolution than a previous model presented by Guerrero-Martínez and Verma (2013). This discretization is intended to approximate more accurately the heat flow in the z-axis and at the same time it allows us to capture the gentle topographic changes of the surface. The resulting mesh accounts for about 8.8×10^6 elements.

$$\nabla \cdot (k \nabla T) = 0 \tag{1}$$

Boundary conditions

$$\frac{\partial T}{\partial x} = 0, \quad \text{for} \quad x = 583340 \quad \text{and} \quad x = 596390$$

$$\frac{\partial T}{\partial y} = 0, \quad \text{for} \quad y = 2196992 \quad \text{and} \quad y = 2212022$$

$$T = 15\ ^{\circ}\text{C}, \quad \text{for} \quad z = \text{surface} \quad \text{and} \quad T = 580\ ^{\circ}\text{C} \quad \text{for} \quad z = \text{Curie Depth}$$

An initial guess for the temperature T was chosen in order to start the simulation. This guess was a geothermal gradient of 80 ºC/km which helped speed up the convergence towards the steady state. The algebraic system was solved with a Gauss-Seidel iteration, which theoretically tends to 0 when the number of iterations is very large. In practice when this method converges behaves asymptotically, the residual of the solution decreases up to certain value which depends on the properties of the matrix of the linear problem (heterogeneity of the problem and mesh size). In this particular problem, at the beginning of the simulations the residual is order 10^3 and it decreases asymptotically up to values of the order 10^{-2}. Although this value can be further decreased a finer numerical discretization would be necessary increasing considerably the computational cost. For this reason, a value of 1.5^{-2} was set as a convergence criterion. In order to speed up the computing process the residual in each iteration was calculated in parallel using OpenMP libraries in Fortran 90. Under these conditions it was required an average of 45 hours of computing time for a simulation case.

6. NUMERICAL RESULTS AND DISCUSSION

Twelve simulation cases consisting of two radii and six depths of the heat sources are considered for this discussion (Table 2). The purpose of evaluating these cases is to determine the sensitivity of the model to the size and depth of the thermal anomalies. The parameters (size of the dikes and depth) that best fit the measured temperatures will be identified.

Table 2: Simulation cases and overall match (ΔT_{mean}) between simulated and measured temperatures for well EAC-1. The best results are highlighted.

Radius (m)	Depth (m bsl)	ΔT_{mean} (ºC)
400	200	9.1
	300	**3.3**
	400	5.5
	500	10.7
	600	15.8
	700	20.6
500	200	30.0
	300	21.7
	400	14.0
	500	7.1
	600	**4.1**
	700	6.4

As mentioned earlier, there are only two temperature logs of exploratory wells available for comparison (EAC-1 and EAC-2). According with the data reported by Lorenzo-Pulido et al. (2011) temperature logs of well EAC-1 were taken 312 hours after drilling was finished, the temperature profile displays an approximately linear trend. In contrast, the available temperature logs for well EAC-2 were taken 24 hours after drilling. Since this time is not long enough to be considered a steady-state temperature profile, only the temperature log of well EAC-1 is used for calibration, whereas well EAC-2 will be considered as a transient temperature profile.

The overall temperature match between simulated and measured temperatures in well EAC-1 is calculated with Equation 2. As shown in Table 2 for heat sources of 400 m radius, 300 m bsl depth (~3100 m bgs) provides the best fit between simulated and measured temperatures with 3.3 ºC of overall deviation. As regards well EAC-2, since it is a transient (cooled down) temperature profile, it is expected to obtain higher simulated temperatures and higher geothermal gradients. The magnitude of this temperature difference can only be known by means of thermal recovery modelling of well EAC-2, for which a drilling record would be necessary.

$$\Delta T_{mean} = \frac{\sum_{i=1}^{n} |T_{log}(z_i) - T_{sim}(z_i)|}{n} \tag{2}$$

Where n is the number depths, z_i, at which temperature logs were taken.

As expected, when the size of heat sources is increased to 500 m radius at the same depth, the thermal impact on the subsurface increases. As a consequence, in order to maintain the fit between simulated and measured geothermal gradients the depth has to increase. For 500 m radius, 600 m bsl depth (~3400 m bgs) turns out the best case.

A direct implication of this behavior is that, for a given temperature of the magma reservoir, a deep heat source is not compatible with

the “swarm of dikes” description of post-caldera magmatism. As the depth increases it is necessary to have a heat source extending over a large area as it would be the case of a single and large magma reservoir.

The 3D temperature field (upper 6000 m) of one of the models that best fit the measured temperatures (400 m radius, 300 m depth. Table 2) is shown in Figure 5. In this configuration of the heat sources the temperature field displays a decrease towards the east and northeast portion of the domain. This gradient can be observed even between the exploratory wells where the isotherms are characterized by a negative slope from EAC-1 to EAC-2. This feature is an evidence of a strongly three-dimensional behavior of the heat flow for this model. Simulated and measured geothermal gradients for this case along with 500 m radius and 600 m depth are shown in Figures 6 and 7, both Figures show possible scenarios for the depth-size relation of the heat source. The curves of both r=400 m and r=500 m show an approximately linear trend up to about 2000 m depth and then a non linear profile as the depth increases due to the thermal anomaly generated by the heat sources. The cases that best fit the measured temperatures of well EAC-1 (Table 2) also display higher geothermal gradients for well EAC-2, as expected in view of the transient nature of this temperature profile. Therefore, for a conductive regime these two cases approximate the thermal field in the subsurface in the vicinity of the exploratory wells, becoming uncertain towards the periphery due to the lack of temperature measurements. Although deeper heat sources underestimate the geothermal gradient of well EAC-1, these cases cannot be disregarded since under deep convective effects they could also lead to higher geothermal gradients in the area.

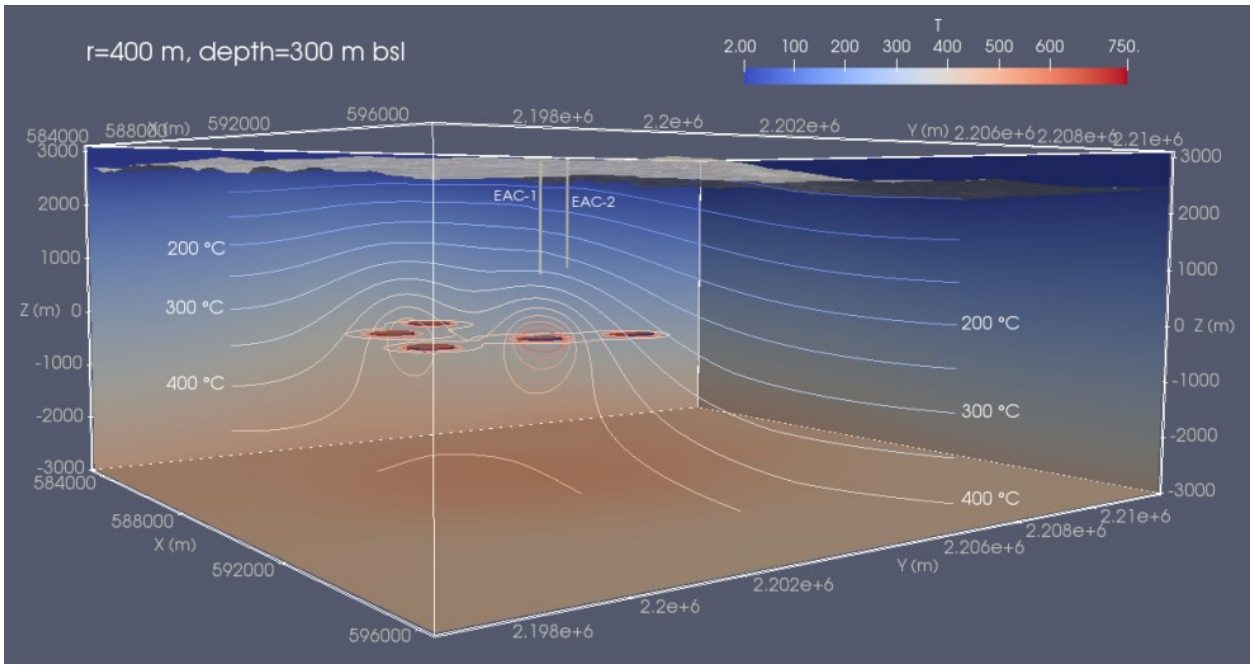

Figure 5: Steady state temperature field of the Ac for heat sources of 400 m radius and 300 m depth bsl.

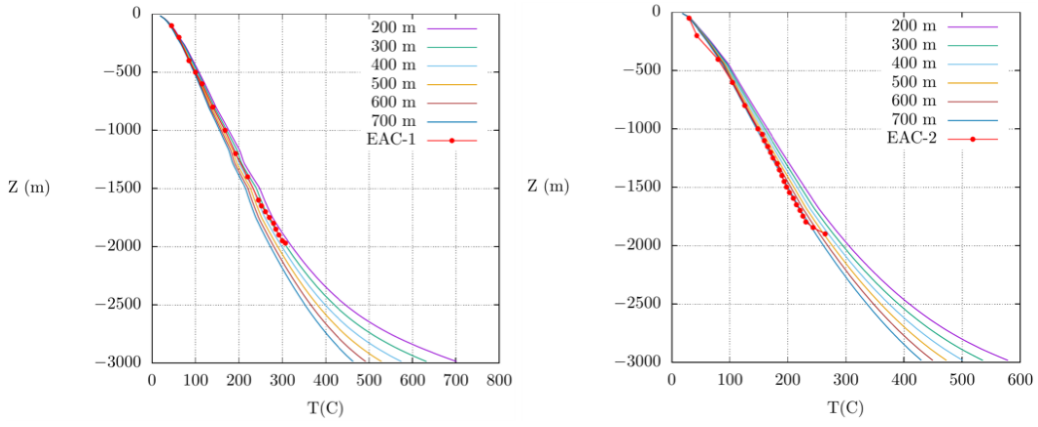

Figure 6: Simulated and measured temperature profiles for heat sources of 400 m radius and six depths. The 3D temperature field for 300 m depth is shown in Figure 5.

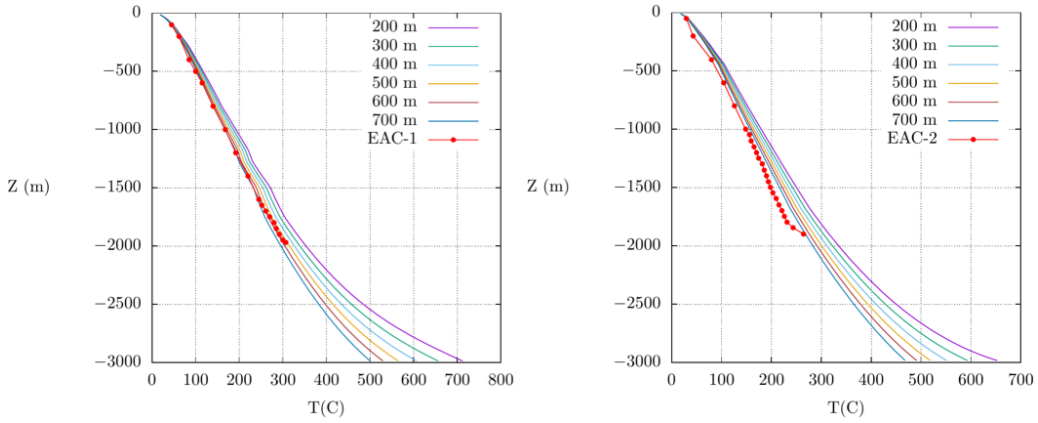

Figure 7: Simulated and measured temperature profiles for heat sources of 500 m radius and six depths.

6. CONCLUSIONS

3D conceptual and numerical models were built for the temperature field of the Acoculco caldera. An estimated Curie isotherm in the area was set as a bottom boundary condition to simulate the background heat flow in the study area. Since the Curie isotherm represents a regional thermal anomaly local heat sources were considered as an additional heat input for the geothermal system. A dikes scheme was chosen to model these thermal anomalies on the basis of recent descriptions of post-caldera magmatism in Acoculco, high temperature intrusive bodies were modeled to attain the geothermal gradients that have been measured in the field. The size and depth of the heat source was varied in a series of simulation cases for calibration with limited temperature logs available. The key findings of the computational simulations presented here can be summarized as follows.

- For a temperature of the magma reservoir of 750 ºC shallow intrusive bodies (3100-3400 m bgs) are required to attain the geothermal gradient that has been measured in the exploratory borehole EAC-1 (138 ºC/km).
- If the depth of the heat source is increased, at the same magma temperature, it is necessary to increase the size too in order to maintain the fit with measured thermal logs, this scenario would not be compatible with recent findings on the post-caldera magmatism that state that the most likely arrangement of the heat source is a swarm of dikes and sills.
- Even though the simulation cases for deep heat sources (>3400 bgs) underestimate the geothermal gradients, these cases cannot be disregarded since under convective effects they could also lead to geothermal gradients as high as the ones measured in the field.
- Modeling the heat source as scattered intrusive bodies give rise to a strongly three-dimensional behavior of the heat flow in the vicinity of the thermal anomaly. This was evident in the temperature drop between wells EAC-1 and EAC-2 for a given depth, even when their separation is of about 500 m. Therefore, it is important to emphasize that the study transient thermal effects should not be restricted to 1D analysis as it has been done in previous thermal models of this caldera.
- It is evident the importance of further exploratory drilling in order to provide a more accurate representation of the structures and their physical properties in the subsurface. Besides, having additional geothermal gradient wells would make possible a more rigorous validation of the background heat flow associated with the estimated Curie isotherm.

These concluding remarks are of clear relevance to provide more accurate representations of the thermal regime of the Acoculco caldera. Furthermore, the numerical model developed here can be an instrument for the assessment of heat flow through the estimation of Curie isotherm in other study areas.

ACKNOWLEDGEMENTS

We acknowledge the financial support by GEMEX, through project number PT5.3.

REFERENCES

Avellán, D.R., Macías, J.L., Layer, P.W., Cisneros, G., Sánchez-Núñez, J., Gómez-Vasconcelos, G., Pola, A., Sosa-Ceballos, G., García-Tenorio, F., Reyes-Austiín, G., Osorio-Ocampo, S., García-Sánchez, L., Mendiola, I.F., Marti, J., López-Loera, H., Benowitz, J., 2018. Geology of the late Pliocene Pleistocene Acoculco caldera complex, eastern Trans-Mexican Volcanic Belt (México). Journal of Maps.

Canet, C., Hernández-Cruz, B., Jiménez-Franco, A., Pi, T., Peláez, B., Villanueva-Estrada, R.E., Alfonso, P., González-Partida, E., Salinas, S., 2015a. Combining ammonium mapping and short-wave infrared (SWIR) reflectance spectroscopy to constrain a model of hydrothermal alteration for the Acoculco geothermal zone, Eastern Mexico. Geothermics 53, 154-165.

Canet, C., Trillaud, F., Prol-Ledesma, R.M., Gonzalez-Hernández, G., Peláez, B., Hernandez-Cruz, B., Sánchez-Córdova, M.M., 2015b. Thermal history of the Acoculco geothermal system, eastern Mexico: Insights from numerical modeling and radiocarbon dating. Journal of Volcanology and Geothermal Research 305, 56-62.

Avendaño-Cortés, J., 2017. Modelo térmico y de conductividad eléctrica en la caldera Tulancingo-Acoculco, Puebla. Master's thesis. Centro de Investigación Científica y de Educación Superior de Ensenada, Baja California.

Finsterle, S., Commer, M., Edmiston, J.K., Jung, Y., Kowalsky, M.B., Pau, G.S.H., Wainwright, H.M., Zhang, Y., 2017. iTOUGH2: A multiphysics simulation-optimization framework for analyzing subsurface systems. Computers & Geosciences 108, 8-20.

Franco, A., Vaccaro, M., 2012. An integrated "Reservoir-Plant" strategy for a sustainable and efficient use of geothermal resources. Energy 37, 299-310.

García-Palomo, A., Macías, J.L., Jiménez, A., Tolson, G., Mena, M., Sánchez-Núñez, J.M., Arce, J.L., Layer, P.W., Santoyo, M.A., Lermo-Samaniego, J., 2018. NW-SE Pliocene-Quaternary extension in the ApanAcoculco region, eastern Trans-Mexican Volcanic Belt. Journal of Volcanology and Geothermal Research 349, 240–255.

Granados-Pastrana, J.E., 2018. Localización de zonas con mayor potencial geotérmico y minero en Acoculco, Puebla. B.S. Thesis. Facultad de Ingeniería, Universidad Nacional Autónoma de México.

Guerrero-Martínez, F.J., Verma, S.P., 2013. Three dimensional temperature simulation from cooling of two magma chambers in the Las Tres Vírgenes geothermal field, Baja California Sur, Mexico. Energy 52, 110-118.

Gutiérrez-Negrín, L., Maya-González, R., Quijano-León, J., 2015. Present situation and perspectives of geothermal in Mexico. Proceedings of the World Geothermal Congress, Melbourne, Australia, 19-25 April 2015 .

López-Hernández, A., Castillo-Hernández, H., 1997. Exploratory drilling at Acoculco, Puebla, Mexico: A hydrothermal system with only nonthermal manifestations. Geohermal Resources Council Transactions 21, 429-433.

López-Hernández, A., García-Estrada, G., Aguirre-Díaz, G., GonzálezPartida, E., Palma-Guzmán, H., Quijano-León, J.L., 2009. Hydrothermal activity in the Tulancingo-Acoculco Caldera Complex, central Mexico: Exploratory studies. Geothermics 38, 279-293.

Lorenzo-Pulido, C., Flores-Armenta, M., Ramírez-Silva, G., 2011. Caracterización de un yacimiento de roca seca caliente en la zona geotérmica de Acoculco, Pue. Geotermia 24, 59-69.

Okubo, Y., Graf, R.J., Hansen, R.O., Ogawa, K., Tsu, H., 1985. Curiepoint depths of the island of Kyushu and surrounding areas, Japan. Geophysics 50, 481–494.

Peiffer, L., Bernard-Romero, R., Mazot, A., Taran, Y.A., Guevara, M., Santoyo, E., 2014. Fluid geochemistry and soil gas fluxes (CO2-CH4-H2S) at a promissory Hot Dry Rock Geothermal System: The Acoculco caldera, Mexico. Journal of Volcanology and Geothermal Research 284, 122-137.

Peiffer, L., Wanner, C., Pan, L., 2015. Numerical modeling of cold magmatic CO2 flux measurements for the exploration of hidden geothermal systems. Journal of Geophysical Research Solid Earth 120, 6856-6877.

Peláez-Pavón, L.B., 2015. Análisis físico-geográfico de la Caldera de Acoculco, Puebla. B.S. Thesis. Facultad de filosofía y letras, Universidad Nacional Autónoma de México.

Sosa-Ceballos, G., Macías, J.L., Avellán, D.R., Salazar-Hermenegildo, N., Boijseauneau-Lopez, M.E., Pérez-Orozco, J.D., 2018. The Acoculco Caldera Complex magmas: Genesis, evolution and relation with the Acoculco geothermal system. Journal of Volcanology and Geothermal Research 358, 288-306.

Stacey, F.D., Banerjee, S.K., 1974. The Physical Principles of Rock Magnetism. Elsevier, Amsterdam.

Thiery, D., Amraoui, N., Noyer, M.L., 2018. Modelling flow and heat transfer through unsaturated chalk Validation with experimental data from the ground surface to the aquifer. Journal of Hydrology 556, 660-673.

Verma, S.P., Gómez-Arias, E., 2016. Flat surface versus present-day topography for cylindrical and spherical sources in temperature field simulation models: The Cerritos Colorados geothermal field, Jalisco, Mexico. Applied Thermal Engineering 107, 70-78.

Versteeg, H.K., Malalasekera, W., 1995. An Introduction to Computational Fluid Dynamics, The Finite Volume Method. Prentice Hall.

Viggiano-Guerra, J.C., Flores-Armenta, M., Ramírez-Silva, G.R., 2011. Evolución del sistema geotérmico de Acoculco, Puebla, México: un estudio con base en estudios petrográficos del pozo EAC-2 y en otras consideraciones. Geotermia: Revista Mexicana de Geoenergía 24, 14-24.

Wong-Loya, J.A., Santoyo, E., Andaverde, J., 2017. A 3-D wellbore simulator (WELLTHER-SIM) to determine the thermal diffusivity of rockformations. Computers & Geosciences 103, 204-214.